DESIGN AND TESTING OF A SESAME COMBINE HARVESTER THRESHING DEVICE / 芝麻联合收获机脱粒装置的设计与试验

Yangyang LI[1)], Dongwei WANG[2)], Abouelnardar SALME[2,3)], Farid Eltom ABDALLAH[2,3)], Kai ZHAO[1)], Zhiguang REN[1)], Zhipeng SUN[1)], Xincheng LI*[1)]

[1)] College of Mechanical and Electrical Engineering, Qingdao Agricultural University, Qingdao / China;
[2)] Yellow River Delta Intelligent Agricultural Machinery Equipment Industry Academy, Dongying / China;
[3)]Academician Workstation of Agricultural High-tech Industrial Area of the Yellow River Delta, National Center of Technology Innovation for Comprehensive Utilization of Saline-Alkali Land, Dongying, Shandong/China
Corresponding author: Xincheng LI
Tel: +86-17630376754; E-mail: 20232111043@stu.qau.edu.cn

DOI: https://doi.org/10.35633/inmateh-78-19

Keywords: *Sesame; Combine harvester; Threshing device; Cylinder; Concave screen; Field test*

ABSTRACT

To address the high threshing loss rate and significant seed breakage during mechanized sesame harvesting, a threshing device suitable for combine sesame harvesters was designed. The threshing characteristics and mechanical requirements of sesame were analyzed, and a method in which threshing drums and concave screens operate in tandem was proposed. Based on the structural parameters of sesame capsules and the requirements of the threshing process, a segmented rib-bar + bar-tooth combination differential drum was designed. The device employs low-speed rib-tooth kneading for threshing, reducing seed damage in the main threshing section, while the high-speed section uses bar-tooth impact action for threshing, reducing seed carryover loss. Field trials were conducted using an innovatively developed sesame combine harvester prototype, with loss rate, impurity content, and seed breakage rate evaluated as key indicators. The results indicate that the designed threshing device achieved a threshing loss rate of 4.09%, a grain breakage rate of 1.98%, and an impurity rate of 1.81%, all meeting the requirements for mechanized sesame harvesting. These findings provide valuable support for the design of combine harvesting equipment for small-seeded crops such as sesame.

摘 要

为解决芝麻机械化收获过程中脱粒损失率高、破碎率大的问题，设计了一种适用于芝麻联合收获机的脱粒装置。调研分析了芝麻作物的脱粒特性及机械脱粒要求，提出了脱粒滚筒与凹板筛协同作业的方法，并基于芝麻蒴果的结构参数和脱粒工艺要求，设计了分段式纹杆+杆齿组合式差速滚筒，装置以低速段纹杆齿的揉搓进行脱粒，降低主脱粒段的籽粒损伤，高速段采用杆齿的打击作用脱粒，降低籽粒的夹带损失率。以损失率、含杂率和籽粒破碎率为指标，通过创新研制的芝麻联合收割机样机开展了田间试验。试验结果表明：所设计的脱离装置脱粒损失率为 4.09%，籽粒破碎率为 1.98%，含杂率 1.81%，均满足芝麻机械化收获作业要求。研究结果可为芝麻等小籽粒作物联合收获装备设计提供支持。

INTRODUCTION

Sesame (*Sesamum indicum L.*), one of China's primary high-quality oilseed crops, saw significant growth in all three key indicators in 2024 compared to 2023, according to data from the National Bureau of Statistics (*Liu et al.,2024*). The total planting area reached 269.39 × 10^5 hectares, with a production volume of 46.75 × 10^4 tons and a yield per unit area of 1,658.31 kg/hectare. Henan, Hubei, and Jiangxi provinces collectively account for over 75% of the national sesame cultivation area and output. However, the uneven plant height, dense capsule distribution, and tendency for capsules to split and shed during harvest result in high labor intensity, low efficiency, and persistently high loss rates. These factors constitute the primary bottlenecks hindering the mechanization of sesame production.

In recent years, numerous scholars have conducted in-depth research on threshing drums to enhance harvesting efficiency and effectiveness, achieving significant progress. For example: Chen Liqing et al. designed a plot breeding threshing system based on a combination of serrated and knife-tooth threshing elements, effectively addressing the high grain breakage rate and incomplete threshing rate during multi-spike wheat threshing operations (*Chen et al., 2025*).

Zhang Hongmei et al., (2025), developed a longitudinal open-flow corn threshing device. Through simulation and experimental parameter optimization, they effectively reduced grain breakage and incomplete threshing rates during corn harvesting, meeting the direct grain harvesting requirements in the Huang-Huai-Hai region.

*Martynas Mili*š*auskas et al., (2025),* studied crop flow control in the longitudinal axial threshing unit during winter wheat harvesting by designing an improved system with 8 synchronously adjustable (10–35°) guide vanes and conducting field comparative tests against the original factory configuration (first 2 fixed + last 6 adjustable) to explore the impact of guide vane adjustment on harvesting performance.

Mohamed Anwer Abdeen et al., (2025), investigated the impact of threshing unit structure and parameters on rice threshing performance by evaluating and optimizing a longitudinal axial flow thresher with conical and drum structures under different rotational speeds and feeding rates, analyzing their effects on throughput, efficiency, seed damage and specific energy.

Vlădut N.-V. et al., (2022), provided relevant achievements in the mathematical modeling of the threshing and separation process in axial flow combines.

Feng Weijing et al., (2024), investigated the single-vertical-axis threshing process based on the viscoelastic damage mechanism of corn kernels, innovatively designing a threshing device suitable for high-moisture corn to effectively optimize operational performance.

Li Ke et al., (2021), designed a high-efficiency, low-damage corn grain direct-harvesting threshing device, resolving issues of high grain damage rates and low cob-cleaning rates caused by unclear threshing mechanisms and suboptimal parameters.

As a core component of combine harvesters, the performance of the separation device directly determines harvesting quality, production efficiency, and economic benefits (*Qu et al., 2025*). Therefore, addressing issues such as high sesame crop carryover loss rate, seed breakage rate, and impurity content, this paper designs a threshing device structure for sesame combine harvesters that integrates a rack-type threshing drum with a long-slot concave screen. It clarifies the primary structural parameters of the drum and the design basis for the concave screen, establishes a model relating drum rotational speed to threshing performance, develops a prototype, and conducts field performance tests. Through measurement and analysis of threshing loss rate, seed breakage rate, and impurity content, the feasibility and effectiveness of this threshing device design were validated.

MATERIALS AND METHODS

Main Structure

The threshing drum of the sesame combine harvester is a key component for separating sesame seeds from their capsules and performing preliminary cleaning. Its structural and operational parameters significantly influence the machine's threshing efficiency, seed breakage rate, and separation effectiveness (*Gu et al., 2025*). Therefore, a well-designed threshing drum can enhance sesame threshing and seed separation performance to a certain extent. The structure of the sesame threshing drum is shown in Figure 1, primarily consisting of a low-speed ribbed roller drum, a high-speed spiked roller drum, a grid-type concave plate screen, and a guide plate assembly.

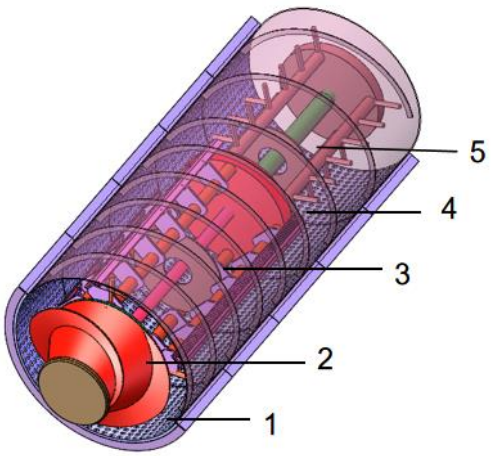

Fig. 1 - Structural Diagram of Sesame Combine Harvester Threshing Unit

1- Grid-format concave plate screen; 2-Concave plate screen spiral conveyor head; 3- Low-speed ribbed rod threshing drum; 4-Deflector plate;5-High-speed spiked tooth threshing drum

This device employs gentle impact and preliminary separation of capsules via the front low-speed roller, followed by enhanced impact and friction from the rear high-speed spiked roller. Combined with the concave plate screen's coordination, it achieves efficient separation of seeds from capsule husks. Simultaneously, the deflector regulates material flow to prevent blockages and reduce grain breakage, thereby ensuring stable and reliable threshing and separation performance of the entire machine (*Chen et al., 2024*).

Working Principle

After being cut by the cutting mechanism, sesame plants are uniformly fed by the feeding device into the low-speed ribbed roller drum at the front end of the threshing mechanism. The drum length matches the width of the feeding device, with multiple sets of ribs arranged axially along the drum wall. The rib surfaces feature spiral-shaped protrusions. Operating at a low rotational speed, the drum applies gentle impact and kneading to the fed plants. This action promotes the initial separation of mature, easily detachable seeds from the capsules under axial thrust and friction. These seeds then fall through the concave plate screen openings into the lower collection trough and are conveyed by a distribution auger to the cleaning system. Incomplete pods and straw continue along the axis under the action of the spiral conveyor.

After exiting the low-speed ribbed drum, the material flows into the rear high-speed spiked drum. Operating at a higher rotational speed, this drum features uniformly distributed spikes that deliver enhanced impact and friction to residual pods, rapidly shattering pod shells and thoroughly detaching adhering grains. The axial thrust within the high-speed drum, combined with the support force from the concave screen, directs the grains through the screen apertures. Meanwhile, straw, empty pod shells, and other impurities are discharged along the drum wall toward the end discharge port (*Mao et al., 2025*).

Design of the Screw Conveyor Head

In the threshing test bench, the threshing drum serves as the core component responsible for the primary threshing task. Within this drum, the spiral conveyor head plays a crucial role in smoothly drawing sesame straw and capsules transported via the bridge conveyor into the threshing chamber. If the auger head is undersized, insufficient material conveying capacity not only prolongs the residence time of sesame within the drum but also causes repeated impacts on the material by the threshing elements, thereby increasing seed damage. Simultaneously, blockages may occur at the bridge outlet and drum inlet, compromising the stability of the device's operation. Therefore, a well-designed auger head can not only reduce seed breakage but also effectively enhance material throughput and operational reliability.

To improve the grabbing and feeding performance of sesame stalks and capsules, this study employs a conical cavity as the main structure with spiral blades welded onto its surface. The number of spiral blades directly impacts feeding uniformity and efficiency: too few blades, especially at low drum speeds, can lead to insufficient feeding, reduced efficiency, and even material accumulation and blockages. Conversely, too many blades at higher speeds may hinder effective material grasping and feeding into the drum. Balancing feeding capacity and seed damage, this study selected two spiral blades as the feeding unit. During operation, the spiral conveyor head rotates counterclockwise, drawing sesame straw and capsules into the threshing chamber. Its contact point with the material can be simplified as a single point O. A force analysis of the interaction between sesame fruit branches and the conveyor head enables further structural optimization, as illustrated in Figure 3.

Fig. 2 - Three-Dimensional Diagram of the Screw Conveyor Head

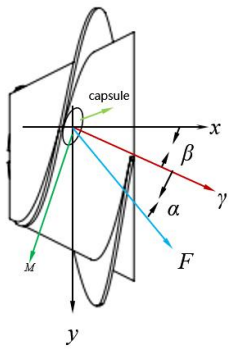

Fig. 3 - Force Analysis Diagram of Sesame

The feeding performance of spiral blades for sesame stalks and capsules is primarily influenced by the helix angle α. Force analysis indicates that sesame material experiences both friction force M and normal thrust γ on the screw blade surface. The angle between the resultant force F and the normal thrust is termed the friction angle β. To ensure smooth conveying, the effective axial thrust of the screw blade must exceed the axial resistance experienced by the material, i.e.:

$$\gamma cos\alpha > M\ sin\alpha \tag{1}$$

where: α is the helix angle (°).

$$M = \gamma\ tan\beta \tag{2}$$

From Equations (1) and (2), the conditions for normal screw conveying are:

$$\alpha < 90 - \beta = 69° \tag{3}$$

To balance conveying capacity and grain damage rate, the helix angle was comprehensively determined to be α=20°. Based on geometric relationships, the length γ_1 of the screw conveyor head can be determined by the following formula:

$$\gamma_1 = \frac{p}{z} \tag{4}$$

where: P represents the screw pitch (taken as 420 mm), and z represents the number of screw heads. Substituting the parameters yields the length of the screw conveyor head:

$$\gamma_1 = 210\ mm \tag{5}$$

Structurally, the conveying head features a conical cavity design with a small-end diameter D1 = 180 mm and a large-end diameter D2 = 300 mm. To ensure smooth flow of sesame seeds into the threshing chamber, the large-end width of the spiral blades is matched to the conical head, designed as W1 = 90 mm, while the small-end width is W2 = 40 mm.

Design of the Threshing Drum

The length and diameter of the threshing drum directly affect its threshing and separation performance. While an excessively long drum can increase feed capacity, it leads to higher energy consumption and grain breakage rates. Conversely, an overly short drum may result in incomplete separation and increased loss rates. Therefore, structural design must balance operational capacity with grain integrity. Referencing relevant domestic and international research findings and the design specifications outlined in JB/T 9778.2-1999 “Design Dimensions and Technical Requirements for Bar-Type Threshing Drums,” and considering the characteristics of sesame seeds-small size, thin seed pods, and fragility-this study determines the drum diameter to be D400 mm. This ensures adequate threshing capacity while minimizing the risk of seed breakage (*Mou et al., 2025*).

The threshing and separation capacity of the drum is primarily determined by its length. Considering sesame plants contain high levels of impurities and seeds are prone to being entrained, the drum is divided into three sections—the feed section, the threshing section, and the separation and impurity removal section—to balance feed intake and cleaning load. As shown in Figure 4.

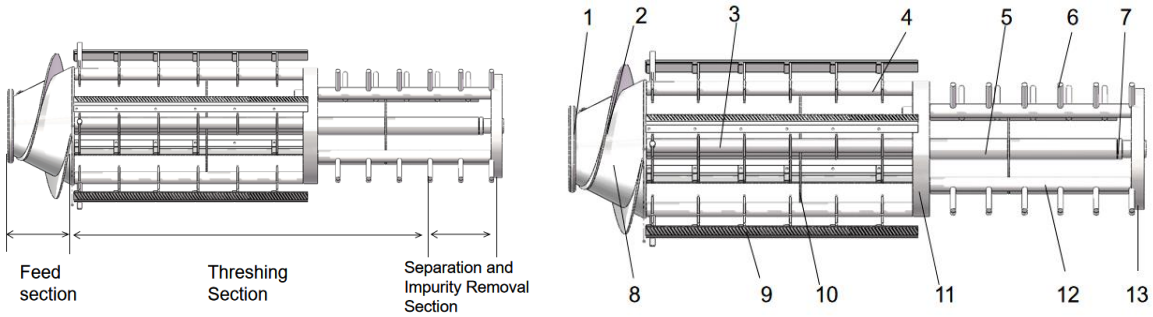

Fig. 4 - Components of the Threshing Drum

1- Front deflector plate; 2-Helical blade; 3-Low-speed shaft; 4-Knurled spoke; 5-High-speed shaft; 6-Pinion gear; 7- High-speed spline sleeve; 8-Helical pusher; 9-Knurled gear tooth; 10-Low-speed disc; 11-Anti-interference retaining ring; 12-Spoke gear tooth; 13-Rear deflector plate

Feed Section: The feed section primarily consists of a screw conveyor head, screw blades, and a front grass deflector plate. The front grass deflector plate is fixed to the frame, serving as a support and guide for the front end of the drum. Sesame plants entering the drum are uniformly pushed toward the threshing section by the screw conveyor head and blades, ensuring even material distribution and reducing accumulation and blockage.

Sesame Threshing Drum: A two-section (front-rear) tandem design. The front section, with patterned rod teeth (12 mm diameter, 60 mm working height, 50Mn steel, 50° inclined alternating left-right helical sawteeth), spokes (4 total) and a low-speed shaft, delivers gentle impact/friction to preliminarily crack capsules and shed seeds. The rear section, equipped with rod teeth, spokes and a high-speed shaft (powered via a spline sleeve), provides high-frequency impact/friction for further seed separation. Operating at 700 r/min (550–750 r/min range) to balance threshing efficiency and seed integrity, the design avoids excessive force-induced breakage while leveraging the seeds' easy-shedding trait. (*Zhao et al., 2025*).

Separation and Impurity Removal Section: This section primarily consists of impurity removal teeth and end caps. The rear grass deflector plate of the end cap is fixed to the frame, providing support and positioning. The impurity removal teeth are mounted on the rod-tooth spokes. As the drum rotates, they facilitate further separation and discharge of impurities from the grains, reducing the workload on the cleaning device. During operation, the threshing drum employs a dual-speed system: the low-speed shaft drives the front drum (ribbed bar section) to rotate at a lower speed, achieving preliminary grain release. The high-speed shaft drives the rear drum to operate at a higher speed, targeting incompletely threshed or stubborn grains. This dual-speed approach ensures overall threshing efficiency and separation effectiveness.

The length of the threshing drum can be calculated using the formula:

$$Y_y s = \frac{1}{\&-\beta}[\&(1-e^{-\beta x}) - \lambda(1-i^{-\&x})] \times 100\% \quad (6)$$

where: $Y_y s$ - grain Separation Rate (%); $\&$ - threshing rate and non-threshing rate ratio coefficient (m^{-1}); β-Probability of grain separation from the screen and coefficient of unsorted grain proportion (m^{-1}); x-Axial position of the roller (m); B - Feed width of the roller (m); L - Drum length (m).

When X = L - B, field trials indicate that threshing loss can be controlled at 5%, achieving a separation rate of 95%. Under optimal seed moisture content conditions for sesame harvesting, model parameters were experimentally determined as λ = 3.8 m^{-1} and α = 3.2 m^{-1}. From this, the following is obtained:

$$L\text{-}B = 1080 \text{ mm} \quad (7)$$

Based on the feed width B=700, the optimal total length of the cross-flow drum can be calculated as:

$$L = 1780 \text{ mm} \quad (8)$$

The calculation results indicate that under the specified conditions, maintaining the drum length within the range of 1.75 m to 1.80 m can effectively balance both the high separation efficiency of sesame seeds and the control of seed breakage rate.

Analysis of Forces on Sesame Capsules and Design of Concave Plate Screen

During the harvest period, the adhesion between sesame seeds and the inner epidermis of the capsule significantly weakens, with the placenta becoming the primary means of attachment (*Zhang et al., 2025*). As the threshing process progresses, the seeds are gradually separated from the capsule. This separation mechanism can be divided into the following stages:

Stage 1: Upon entering the threshing chamber, sesame capsules are subjected to the force exerted by the threshing elements and the counterforce from the concave screen.

Stage 2: Under the combined action of the threshing elements and the concave screen's counterforce, the capsule's outer pericarp first cracks at the attachment points, initiating the separation of seeds from the placenta.

Stage 3: As impact and friction continue, the pod shell progressively fractures. The bond between seeds and placenta weakens further, with some seeds achieving complete separation.

Stage 4: The capsule shell completely ruptures, and the seeds are fully separated from the placenta. During this process, the seeds are not only struck by the threshing elements but also interact with capsule fragments and other seeds, ultimately achieving the separation of most seeds, as shown in Figure 5.

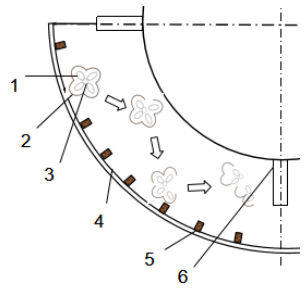

Fig. 5 - Analysis of Sesame Capsule Threshing

1-Sesame seed kernel; 2-Outer seed coat; 3-Placenta; 4-Concave sieve plate; 5-Crossbar; 6-Threshing element

This separation mechanism indicates that the structural parameters of the concave screen directly influence the threshing efficiency of sesame seeds. Rational design of the screen aperture shape, aperture size, and open area ratio not only facilitates smooth passage of seeds but also reduces secondary compression and breakage during separation. This approach ensures separation efficiency while minimizing seed damage rates (*Gao et al.,2024*).

Sesame threshing primarily relies on the coordinated action of threshing elements within the drum and the concave screen. Through impact, collision, and friction, the seeds are separated from the capsules. Upon colliding with the cross-bar, the capsules rupture, releasing the seeds which are then separated through the screen apertures. Due to the small size of sesame seeds, the structural design of the concave plate screen significantly impacts separation efficiency and seed damage: excessively large screen apertures hinder effective separation of seeds from impurities, increasing contamination rates; conversely, overly small apertures reduce effective screening area, leading to poor seed throughput at high feed rates and increased carryover losses. Figure 6 illustrates the force analysis of sesame capsules within the drum.

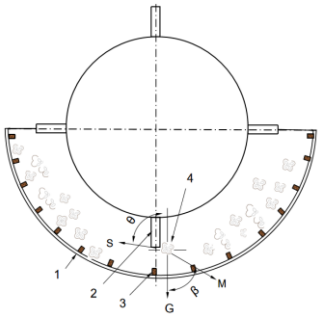

Fig. 6 - Stress Analysis Diagram of Sesame Capsule and Transverse Septum

1-Concave Screen Mesh; 2-Threshing Element; 3-Crossbar;4-Sesame Capsule Model

Vertical force analysis during collision between sesame capsule and diaphragm:

$$S\cos\theta = M\cos\beta + G \tag{9}$$

$$\cos\theta \approx \frac{r-h}{r} \tag{10}$$

where: S - shear force (N) exerted on the sesame capsule by the transverse partition; M - Impact force exerted by the threshing unit on sesame capsules (N); G - gravitational force acting on sesame capsules (N) ;r - sesame capsule radius (mm); h - height of the crossbar above the screen mesh (mm); β - the angle (°) between the impact force M exerted by the threshing component on the sesame capsule and the vertical direction; θ - angle (°) between the shear force S applied to the sesame capsule and the vertical direction.

From Equations (9) and (10), the following is obtained:

$$S = \frac{(M\cos\beta + G)r}{r-h} \tag{11}$$

Since the radius r of the sesame capsule, the angle β between the impact force from the threshing element and the vertical direction, and the angle θ between the shear force S and the vertical direction are all fixed during the threshing process, and the impact angle β applied to the sesame capsule is also a constant value, the magnitude of the shear force S is closely related to the protrusion height h of the crossbar.

When height h increases, the shear force S on the seed pods intensifies, making the seeds more prone to breakage and increasing the breakage rate. Conversely, when height h decreases, the shear force S diminishes, reducing seed damage and lowering the breakage rate. Therefore, in the design of concave screens, appropriately reducing the height h of the crossbar can decrease the breakage rate of sesame seeds (*Wang et al., 2024*).

Concave Plate Screen Structure Types

(1) The concave screen is the key component for separating grains from impurities, positioned beneath the threshing drum. The metric that indicates the concave screen's performance is called the screen opening rate, calculated using the following formula:

$$\beta = \frac{A_{Total\ sieve\ opening\ area}}{A_{Total\ area\ of\ concave\ screens}} \quad (12)$$

where: β represents the screen aperture rate, %. The screen aperture rate is positively correlated with the effective fruit-picking area, resulting in superior separation efficiency. Depending on their screen surface structure, concave screens are categorized into grid-type, perforated-type, and woven-type. The advantages, disadvantages, and application ranges of these three concave screens are summarized in Table 1.

Table 1

Advantages, Disadvantages, and Applications of Concave Plate Screens

Types	Advantages	Disadvantages	Scope of Application
Grid-type Concave Plate Screen	Wide applicability, excellent separation efficiency, high screening rate, high strength, minimal entrainment loss	Highly damaging	Combine harvester
Punch-type concave plate screen	Simple structure, low friction	Prone to wear and deformation, short service life, prone to residue buildup at junctions, prone to clogging	Less commonly used
Woven Concave Screen	Easy to process, low friction, excellent wear resistance	Low separation efficiency, low screen open area ratio	Less commonly used

After comparing the advantages and disadvantages of the three methods, considering the large sesame seed feed rate and the high requirements for separation performance, this study adopted a grid-type concave plate screen.

(2) Structural Parameter Design

Enveloping Angle: The working area of concave plate screens directly impacts separation capacity, while the size of the enveloping angle determines its effective separation area. Increasing the enveloping angle enhances separation efficiency and reduces entrainment loss, but beyond a certain range, the improvement becomes limited. Based on the screening probability model per unit shaft length, the analytical relationship between the enveloping angle and the target separation rate is:

$$\beta = -\frac{1}{\lambda R} 1n(1 - P_S) \quad (13)$$

where: β-represents the wrap angle of the concave plate screen (°); λ-the probability density of grain being screened out per unit axial length is constant (m^{-1}); R-drum radius (m); Ps-target separation rate (%)

Substituting the experimental fitting value λ = 3.8 m^{-1} and drum radius R = 0.2 m, the design range for the wrap angle β is 180° to 230°. This yields a theoretical separation rate of 90% to 95%. This study selected 225°, achieving a separation rate of approximately 95%.

Screen aperture size: Given that sesame seeds measure approximately 3.08 mm in length, excessively large apertures may allow stems and pod fragments to enter the grain bin, increasing impurity levels. Conversely, overly small apertures reduce screening efficiency, impede seed flow, and increase entrapment losses. Comprehensively considering passability and separation efficiency, this study designed a screen aperture of 5 mm × 12 mm. This size ensures smooth grain passage while effectively blocking most stems and pod fragments (*Luo et al., 2024*).

In summary, employing a grid-type concave plate screen with a 225° wrap angle and 5 mm × 12 mm apertures, while controlling grain breakage rate by reducing the protrusion height of the crossbar, can simultaneously ensure separation efficiency and reduce impurity content and damage rates. As shown in Figure 7.

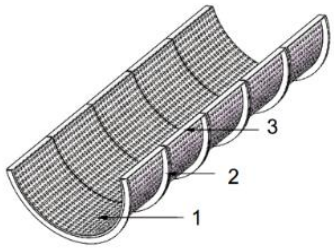

Fig. 7 - Schematic Diagram of Concave Plate Screen Structure
1-Screen Mesh; 2-Curved Plate; 3-Cross-Bracing Plate

Top Cover and Deflector Plate Design

In the traditional sesame threshing drum cover structure, guide plates are typically arranged uniformly, primarily serving to regulate the direction and speed of material movement within the threshing chamber. However, this uniform arrangement exhibits significant shortcomings in practical operation. On one hand, the front section of the drum experiences concentrated material inflow, making it difficult for the guide plates to rapidly disperse and convey the material. This often leads to inlet blockages and accumulation, disrupting continuous and stable operation. On the other hand, the material moves too rapidly in the rear section of the drum, resulting in insufficient dwell and kneading time. This causes incomplete seed separation, thereby reducing threshing quality (*Wang et al., 2023*).

To address these issues, this study proposes a zoned guide plate arrangement: high-density (150 mm pitch) in the front to speed up material flow, improve initial threshing efficiency, and prevent blockages; low-density (250 mm pitch) in the rear to slow axial velocity, extend separation time, and enhance seed separation and passage through the concave screen, as shown in Figure 8.

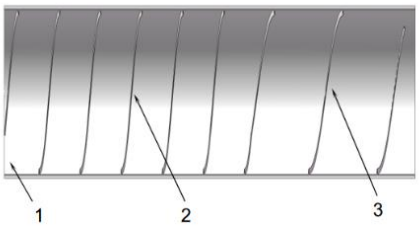

Fig. 8 - Threshing Drum Guide Plate
1-Top cover; 2-High-density spiral guide plate; 3-Low-density spiral guide plate

This combination of high-density front-end and low-density rear-end deflector plates balances clog resistance with separation quality. It not only resolves the issues of front-end clogging and incomplete rear-end separation inherent in traditional uniform deflector plate arrangements but also reduces grain breakage rates and cleaning burdens to a certain extent. Consequently, it significantly enhances the overall efficiency and stability of the threshing mechanism (*Mousa et al.,2022*).

RESULTS

Test Conditions

Field trials were conducted at the experimental plots of the Yellow River Delta Intelligent Equipment Industry Research Institute, with soil moisture content at approximately 16.8%. The sesame variety used was “Luzi No. 3,” sown in May 2023 and reaching optimal harvest maturity in late September. At harvest, the sesame seeds had an average moisture content of 11%, with plant heights ranging from 110–130 cm. The average triaxial dimensions of the seeds were 3.2 mm × 2.1 mm × 1.5 mm.

Throughout the trial period, the surface soil moisture content remained at 16.8%. The crop stand exhibited uniform maturity, and seed moisture content was within the optimal harvesting range, minimizing experimental variability caused by moisture differences. To ensure sampling and measurement accuracy, the implement working width was set at 2.5 m, with each pass covering 30 m, thereby defining a single harvest

area of 60 m² as the basic test unit. The experiment was repeated across multiple randomly selected harvest units to minimize plot variation and environmental influences, enhancing the reliability and representativeness of the results (*Liu et al., 2022*).

Regarding the parameter settings, to ensure comparability across trials, the threshing drum speed was uniformly set to 650 r/min, with a drum-concave gap of 30 mm. These operating conditions satisfied the separation requirements for sesame seeds and capsules while minimizing excessive seed damage, providing a stable basis for subsequent performance evaluation. Field trials are illustrated in Figure 9.

Fig. 9 - Field Trial Photograph

Field Trials and Results

Entrained Loss Rate

The carryover loss rate is a key indicator for evaluating the threshing and separation performance of harvesters. It primarily reflects the extent to which grains fail to separate completely after passing through the threshing mechanism and are discharged alongside straw or debris. An elevated carryover loss rate indicates insufficient separation efficiency, resulting not only in grain loss but also increasing the workload for subsequent cleaning operations (*Yu et al., 2021*).

During machine operation, materials discharged from the straw outlet and grains discharged from the rear end are collected separately. Through manual screening and sorting, the mass of grains is weighed. Combined with the mass of grains collected in the grain bin, the formula for calculating the carryover loss rate is:

$$S_j = \frac{N_P}{N_P + N_O + N_I} \times 100\% \quad (14)$$

where: N_P - mass of seeds entrained at the straw discharge port (kg); N_O - grain quality discharged from the rear of the machine (kg); N_I - grain weight in the silo (kg); S_j - Sesame Loss Rate (%).

The test results are shown in Table 2.

Table 2

Determination of Drag Loss Rate in Field Trials

Harvesting Unit	Total mass of sesame seeds (kg)	Total Sesame Seed Mass at the Straw-Removal Port (kg)	Sesame Loss Rate (%)
1	12.65	0.21	1.66
2	13.24	0.25	1.88
3	11.26	0.18	1.59
4	12.10	0.24	1.98
5	12.54	0.26	2.07
6	11.36	0.21	1.84
7	12.61	0.25	1.98
8	13.14	0.19	1.44
9	12.69	0.23	1.81
average	111.59	2.02	1.81

Under the operating conditions established in this research institute, the measured average grain carryover loss rate was 1.81%.

Crushing Rate

The breakage rate is one of the key indicators for assessing grain harvest quality (*Hao et al., 2022*). Sesame seeds are small in size with thin seed coats, making them highly susceptible to cracking or damage during threshing due to drum impact or friction and compression between materials. Excessive breakage not only reduces seed value but also impacts subsequent oil extraction quality, necessitating strict control.

In the experiment, samples were randomly collected from the upper, middle, and lower sections of the grain silo, with 500 g of seeds taken from each location. A total of 4500 g was used as the analysis sample. Damaged seeds were manually sorted out, weighed, and the breakage rate was calculated using the formula:

$$S_p = \frac{Z_1 + Z_2 + Z_3}{500} \times 100\% \quad (15)$$

where: Z_1, Z_2, Z_3 - represent the mass (g) of broken grains in the upper, middle, and lower layers of the sample, respectively; S_P - Sesame Crushing Rate.

The test results are shown in Table 3.

Table 3

Determination of Sesame Loss Rate in Field Trials

Harvesting Unit	Sample Mass (g)	Sesame Sample Crushing Quality (g)	Sesame Crushing Rate (%)
1	500	24.62	4.92
2	500	25.12	5.02
3	500	21.58	4.31
4	500	24.39	4.87
5	500	21.32	4.26
6	500	22.69	4.53
7	500	23.65	4.73
8	500	20.99	4.19
9	500	21.54	4.31
average	4500	205.93	4.58

Under uniform drum speed of 650 r/min and a drum-to-concave gap of 30 mm, the measured average grain breakage rate was 4.58%.

Impurity Content

The impurity rate indicates the proportion of post-harvest grain stored in silos that contains stem debris, empty husks, soil clods, stones, and other contaminants relative to the total sample weight (*Wang et al.,2021*). It serves as a key indicator for evaluating the quality of harvesting, threshing, and preliminary separation processes, as illustrated in Figure 10.

Fig. 10 - Sesame Seeds with Impurities

The trial was conducted using a single working area of 60 m² as the basic unit. After each machine completed operations in each test plot, samples were randomly collected from the upper, middle, and lower layers of the grain bin. Three separate samples were taken from each layer for weighing, with each layer yielding 500 g of sample material. A total of 4500 g was collected as the test sample. Simultaneously, collect and weigh the impurities discharged from the straw outlet and rear end to determine the impurity rate, as shown in Figure 10.

The formula for calculating the impurity rate is:

$$S_P = \frac{M_N}{M_E} \times 100\% \quad (16)$$

where: M_N - mass of stem debris, empty seed pods, soil, stones, etc. (g); M_E - total sample mass (g); S_P - impurity content.

Table 4

Determination of Impurity Content in Field Trials

Harvesting Unit	Sample Mass (g)	Stem debris (g)	Empty seed pod (g)	Pebble (g)	Impurity Content (%)
1	500	5.95	3.01	0.15	1.82
2	500	5.52	3.69	0.13	1.86
3	500	5.94	2.54	0.16	1.72
4	500	6.01	3.05	0.12	1.83
5	500	6.39	2.59	0.14	1.82
6	500	6.05	3.04	0.11	1.84
7	500	5.68	2.57	0.18	1.68
8	500	6.53	2.31	0.14	1.79
9	500	6.39	3.28	0.12	1.95
average	4500	54.1	26.08	1.25	1.81

Field trials revealed that the sesame combined harvesting and threshing device exhibited a carryover loss rate of 1.81%, a loss rate of 4.58%, and an impurity rate of 1.81%.

CONCLUSIONS

(1) To address the characteristics of sesame capsules - such as their tendency to split, small seed size, and susceptibility to breakage - a segmented ribbed rod + rod-tooth combination differential drum was designed. The device utilizes the kneading action of low-speed segment ribbed teeth for threshing, reducing seed damage in the primary threshing section. The high-speed segment employs the impact action of rod teeth for threshing, minimizing seed carryover loss rates. The drum diameter is 400 mm, total length is 1.78 m, and operating speed is controlled around 650 r/min. The concave screen has a wrap angle of 180°, with screen apertures of 4 mm × 12 mm. It employs a “high-density front section (pitch 150 mm) + low-density rear section (pitch 250 mm)” guide plate layout, achieving a “gentle impact – deep kneading separation” operating mode.

(2) Field validation conducted at the Yellow River Delta experimental farm in Dongying, Shandong Province demonstrated: under grain moisture content of approximately 11%, the device exhibited stable performance with an average threshing loss rate of 1.98%, grain breakage rate of 4.09%, and impurity content of 1.81%. All metrics fell below national limits for small-grain crop combine harvesters, meeting agronomic requirements for sesame harvesting.

(3) Compared to traditional uniform guide plate layouts, the proposed “zonal guide plate + ribbed bar structure” significantly mitigates issues such as front-end blockage and incomplete rear-end separation. This design reduces grain secondary impact and breakage probability while enhancing threshing and separation efficiency.

ACKNOWLEDGEMENT

We sincerely thank the anonymous reviewers and editors for their rigorous and meticulous review. This research was supported by the Shandong Provincial Base and Talent Program (“Foreign Experts Double Hundred Plan” Talent Category) (WSR2023093).

REFERENCES

[1] Ali Khaled Abdeen Mousa, Zong Wang Yuan, Ma Li Na, Abd El Wahhab Gomaa Galal & Li Mao. (2022). Testing, Evaluating and Simulate the Performance of the Newly Designed Drum for a Sunflower Threshing Machine. *International Journal of Engineering Research in Africa, 6537,* 29-41.

[2] Chen Liqing, Zhu Junwen, Liu Ce, Zhang Chunling, Zhang Haotian & Cai Zengbin. (2025). Optimized Design and Testing of a Threshing Device for Wheat Breeding Plots（*小麦小区育种脱粒装置优化设计与试验*）. *Transactions of the Chinese Society for Agricultural Machinery*, 56(07), 72-81.

[3] Fazheng Wang, Yanbin Liu, Yaoming Li & Kuizhou Ji. (2023). Research and Experiment on Variable-Diameter Threshing Drum with Movable Radial Plates for Combine Harvester. *Agriculture, 13* (8),

[4] Feng Weijing. (2024). *Study on the Mechanism of Viscoelastic Collision Damage in Corn and the Development of a Dehulling Device*（玉米粘弹性碰撞损伤机理及脱粒装置研究）(Master's Thesis, Jilin University).

[5] Gao Pengfei, Zhang Xinwei, Jiang Chunxia, Yi Kechuan, Zhang Xiaolong & Ma Zhanwei. (2024). Optimized Design and Testing of an Axial Roller-Type Sweet Corn Sheller *(轴向滚筒式鲜食玉米脱粒装置优化设计与试验)*. *Transactions of the Chinese Society for Agricultural Machinery*, 55 (S2), 145-156.

[6] Hao, J. J., Wei, W. B., Qin, J. H., Zhu, Z. M., Lü, X. Y., & Yang, S. H. (2022). Design and testing of a cut-flow sunflower threshing and screening machine *(切流式油葵脱粒筛分机设计与试验)*. *Transactions of the Chinese Society of Agricultural Machinery*, 53(02), 139-148.

[7] Liu Aihua, Ye Liqi, Editors-in-Chief. (2024). Editorial Board and Editorial Staff of the China Statistical Yearbook 2024. Liu Aihua, Ye Liqi, Editors-in-Chief (eds.). *China Statistical Yearbook* (*中国统计年鉴*) China Statistics Press, pp. 4–5.

[8] Linfeng Chen, Lei Zhang, Le Li & Lihua Zhang. (2024). Design and Experiment of a Low-Damage Threshing Drum for Corn with Stepless Taper Adjustment. *Agriculture, 15* (1), 4-4.

[9] Martynas Milišauskas, Niels Petersen, Greta Milišauskienė, Mantas Petrulis, Dainius Savickas. Crop Flow Control in a Longitudinal Axial Threshing Unit Using Fully Adjustable Guide Vanes: A Field Study in Winter Wheat Harvesting[J]. *Applied Sciences*, 2025, 15 (12):

[10] Mao Xin, Li Yuanchao, Yi Shujuan, Zhang Dongming, Wang Guangyu & Wang Peng. Design and Testing of Threshing Components for a Corn Axial Flow Threshing Device *(玉米轴流脱粒装置脱粒元件的设计与试验)*. *Agricultural Mechanization Research*, 1-9.

[11] Mou Chende & Guo Lianhu. (2025). Research on the Optimized Design of Combine Harvester Threshing Devices *(联合收割机脱粒装置优化设计研究)*. *Agricultural Machinery*, (06), 141-143.

[12] Mohamed Anwer Abdeen, Weibin Wu, Abouelnadar El Salem, Ahmed Elbeltagi, Ali Salem, Khaled A Metwally, Guozhong Zhang, Abdallah Elshawadfy Elwakeel. The impact of threshing unit structure and parameters on enhancing rice threshing performance [J]. *Scientific reports*, 2025, 15 (1):

[13] Qu Wanwan & Li Jing. (2025). Optimized Design and Testing of a Corn Dehulling Device *(玉米脱粒装置的优化设计与试验)*. *China Agricultural Machinery Equipment,* (09), 79-82.

[14] Li Ke. (2021). *Design and Experimental Study of a Vertical-Flow Corn Grain Direct-Harvest Threshing Device*（纵轴流玉米籽粒直收脱粒装置的设计与试验研究）(Master's Thesis, Shandong Agricultural University).

[15] Liu Yanbin, Li Yaoming, Dong Yunhua, Huang Mingsen, Zhang Tao & Cheng Junhui. (2022). Development of a variable-diameter threshing drum for rice combine harvester using MBD - DEM coupling simulation. *Computers and Electronics in Agriculture, 196*.

[16] Shao Yongming. (2020). *Design and Experimental Study of Low-Damage Threshing Equipment for Corn Grain Harvesters*（玉米籽粒收获机低损伤脱粒装备设计与试验研究）(Master's Thesis, Anhui University of Science and Technology).

[17] Vlădut N.-V., Biris S.St., Cârdei P., Găgeanu I., Cujbescu D., Ungureanu N., Popa L.-D., Perişoară L., Matei G., Teliban G.-C. (2022). Contributions to the Mathematical Modeling of the Threshing and Separation Process in An Axial Flow Combine. *Agriculture*, 12(10), 1520.

[18] Wang Fanrui, Li Bin, Zhu Rongguang, Wang Shiguo, Liu Yang, Gao Xiaolong & Yang Xingyu. (2024). Design and Testing of an Air-Screen Cleaning Device for Cumin Threshers *(孜然脱粒机风筛式清选装置的设计与试验)*. *Transactions of the Chinese Society for Agricultural Engineering*, 40(22), 39-50.

[19] Wang Hao, Ba Xinyi, Zheng Decong, HUSSAIN Saddam, Wang He, & Song Haiyan. (2021). Design and Simulation of a Clean Threshing Device for Buckwheat *(荞麦洁净式脱粒装置设计与仿真)*. *Agricultural Engineering*, 11(09), 84-88.

[20] Xinyang Gu, Bangzhui Wang, Zhong Tang, Honglei Zhang & Hao Zhang. (2025). Automatic Vibration Balancing System for Combine Harvester Threshing Drums Using Signal Conditioning and Optimization Algorithms. *Agriculture*, 15 (14), 1564-1564.

[21] Zhang Hongmei, Hu Jingying, He Xun, Qu Zhe, Yang Liquan, Li Shilong & Zhang Jing. (2025). Optimized Design and Testing of a Vertical Axial Flow Open-Type Corn Threshing Device *（基于纵轴流开式玉米脱粒装置的优化设计与试验）*. *Journal of Henan Agricultural University*, 59 (01), 122-135.

[22] Zhao Zhenhua, Zhang Yuan, Shen Dezhan & Wei Lijiao. (2025). Structural Design and Testing of a Centrifugal Pepper Threshing Device*(离心式胡椒脱粒装置结构设计与试验)*. *Chinese Journal of Agricultural Machinery Chemistry*, 46 (09), 23-30+57.

[23] Zhang Ligong. (2025). Research and Testing on Combined Cutting Flow and Longitudinal Axial Flow Threshing Separation Device for Combine Harvesters*(联合收割机切流+纵轴流脱粒分离装置研究与试验)*. *Agricultural Machinery*, (03), 47-52.

[24] Zengjia Luo, Jinliang Gong & Yanfei Zhang. (2024). Reliability Analysis and Optimization of Corn Threshing Drum Based on Kriging Approximation Model. *Journal of Biosystems Engineering, 49* (4), 1-12.

[25] Zhiwu Yu, Yaoming Li, Xinzhong Wang, Zhong Tang & Lu Jiahui. (2021). Effects of Side Load Chains of a Combine Harvester on Unbalanced Dynamic Vibrations of Its Threshing Drum. *International Journal of Rotating Machinery,* 2021，8896349.